VEHICLE WHEEL-GROUND CONTACT ANGLE ESTIMATION: WITH APPLICATION TO MOBILE ROBOT TRACTION CONTROL

K. IAGNEMMA
S. DUBOWSKY
Massachusetts Institute of Technology, Cambridge, MA USA
email: kdi@mit.edu

Abstract. Knowledge of wheel-ground contact angles in vehicles, and in particular mobile robots, is an essential part of many traction control algorithms. However, these angles can be difficult to measure directly. Here, a method is presented for estimating wheel-ground contact angles of mobile robots using commonly available on-board sensors. The method utilizes an extended Kalman filter to fuse noisy sensor signals. Simulation and experimental results from a six-wheeled mobile robot demonstrate the effectiveness of the method.

1. Introduction

Current paradigms for planetary exploration are strongly dependent on small wheeled robots ("rovers") to seek out and retrieve scientific information (Hayati *et al*, 1996). The recent Pathfinder mission is a successful example of the capabilities of such systems (Mishkin *et al.*, 1998). However, the scope of the Pathfinder mission was limited to short traverses in relatively benign terrain. In future missions, rovers will be required to negotiate increasingly challenging terrain to achieve science objectives (Hayati *et al*, 1996). To ensure rover safety and enhance performance, advanced control techniques such as traction control will be required (Sreenivasan and Wilcox, 1994; Farritor *et al.*, 1998). An important variable for many traction control algorithms is the wheel-ground contact angles (Sreenivasan and Wilcox, 1994; Farritor *et al.*, 1998). These angles influence vehicle weight distribution, which strongly affects wheel traction. Unfortunately, these angles are difficult to measure directly. In this paper, a method is presented for estimating wheel-ground contact angles of mobile robots using readily-available on-board sensors.

In an attempt to measure contact angles, researchers have proposed installing multi-axis force sensors at each wheel to measure the contact force direction (Sreenivasan, 1994). The wheel-ground contact angles could

be inferred from the direction of the contact force. However, installing multi-axis force sensors at each wheel is costly and mechanically complex. The complexity reduces reliability and adds weight, two factors that carry severe penalties for space applications.

The algorithm presented in this paper is based on rigid-body kinematic equations and uses simple sensors such as vehicle inclinometers and wheel tachometers. It does not require the use of force sensors. The method utilizes an extended Kalman filter to fuse noisy sensor signals. Simulation and experimental results using a six-wheeled rover show the effectiveness of the method.

2. Wheel-Ground Angle Equations

Consider the planar two-wheeled system on uneven terrain, shown in Figure 1. The system is assumed to be skid-steered. The wheel-ground contact angles in the direction of travel of the vehicle are considered. The transverse contact angles are not considered, as this angle information would not be used by the traction control system for such a system. The ground is assumed to be rigid, and the wheels are assumed to make contact with the ground at a single point.

As shown in Figure 1, the rear and front wheels make contact with the ground at angles γ_1 and γ_2 from the horizontal, respectively. The vehicle pitch, α, is also defined with respect to the horizontal. The wheel centers have speeds v_1 and v_2. These speeds are in a direction parallel to the local wheel-ground tangent plane due to the rigid ground assumption. The distance between the wheel centers is defined by l.

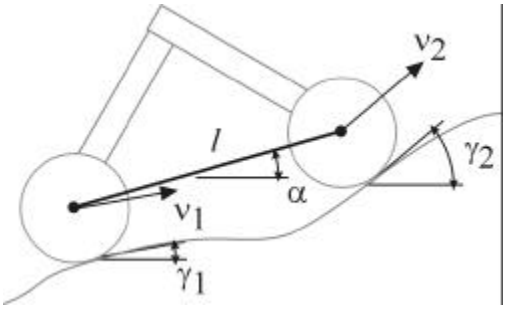

Figure 1. Planar two-wheeled system on uneven terrain

For this system, the following kinematic equations can be written:

$$v_1 \cos(\gamma_1 - \alpha) = v_2 \cos(\gamma_2 - \alpha) \tag{1}$$

$$v_2 \sin(\gamma_2 - \alpha) - v_1 \sin(\gamma_1 - \alpha) = l\,\dot{\alpha} \tag{2}$$

Equation (1) represents the constraint that the wheel center length l does not change. Equation (2) is a rigid-body kinematic relation between the velocities of the wheel centers and the vehicle pitch rate $\dot{\alpha}$.

Combining Equations (1) and (2) results in:

$$\sin(\gamma_2 - \alpha - (\gamma_2 - \alpha)) = \frac{l\,\dot{\alpha}}{n_1}\cos(\gamma_2 - \alpha) \tag{3}$$

With the definitions:

$$\theta \equiv \gamma_2 - \alpha, \quad \beta \equiv \alpha - \gamma_1, \quad a \equiv l\,\dot{\alpha}/n_1, \quad b \equiv n_2/n_1$$

Equations (3) and (1) become:

$$(b\sin\theta + \sin\beta)\cos\theta = a\cos\theta \tag{4}$$

$$\cos\beta = b\cos\theta \tag{5}$$

In most cases Equations (4) and (5) can be solved for the ground contact angles γ_1 and γ_2 as:

$$\gamma_1 = \alpha - \cos^{-1}(h) \tag{6}$$

$$\gamma_2 = \cos^{-1}(h/b) + \alpha \tag{7}$$

where:

$$h \equiv \frac{1}{2a}\sqrt{2a^2 + 2b^2 + 2a^2b^2 - a^4 - b^4 - 1}$$

There are three special cases that must be considered. The first special case occurs when the vehicle is stationary. In this case Equations (6) and (7) do not yield a solution. This results from the fact that a robot in a fixed configuration can have an infinite set of possible contact angles at each wheel.

The second special case occurs when cosθ is equal to zero. This corresponds to the case where the front wheel contact angle is offset by $\pm\pi/2$ radians from the pitch angle, such as when a vehicle on flat terrain encounters a vertical obstacle. In this case, the motion of the vehicle can be viewed as pure rotation about a point fixed at the rear wheel center (see Figure 2). Equation (4) then degenerates, and the system is unsolvable. However, Equations (1) and (2) can be simplified by the observation that n_1 is zero, and the kinematic equations can be written as:

$$v_2\cos(\gamma_2 - \alpha) = 0 \tag{8}$$

$$v_2\sin(\gamma_2 - \alpha) = l\,\dot{\alpha} \tag{9}$$

The variable g_1 is undefined in Equations (8) and (9) since the rear wheel is stationary, and:

$$g_2 = a + \frac{p}{2}\text{sgn}(\dot{a}) \tag{10}$$

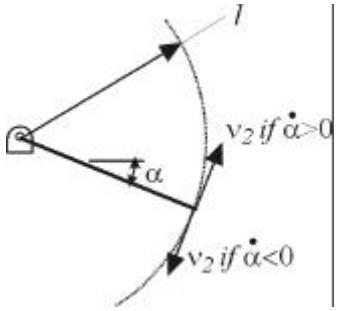

Figure 2. Kinematic description of case where $\cos q = 0$

The third special case occurs on terrain where the front and rear wheel-ground contact angles are identical (see Figure 3a-c). In this case the pitch rate $\dot{a}$ is zero and the ratio of n_2 and n_1 is unity. This implies that the quantity h in Equations (6) and (7) is undefined and the system of equations has no solution. However, it should be noted that the ground contact angle equations are expressed as functions of the vehicle pitch and pitch rate, a and $\dot{a}$, and the wheel center speeds, n_1 and n_2. The pitch and pitch rate can be physically measured with rate gyroscopes or inclinometers. The wheel center speeds can be estimated with knowledge of the wheel angular rate. Thus it is trivial to detect the case of flat terrain (Figure 3a) when the pitch angle a is constant, and the contact angles are equal to the pitch angle.

In cases such as in Figure 3b and Figure 3c, it can be assumed that if the terrain profile varies slowly with respect to the data sampling rate, the ground contact angles will change slowly from the previously computed ground contact angles. Thus, previously estimated ground contact angles can be used in situations where a solution to the estimation equations does not exist.

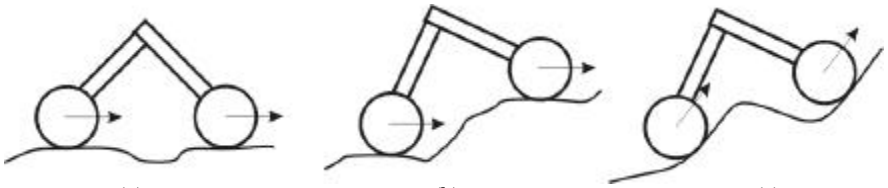

(a) *(b)* *(c)*

Figure 3. Examples of terrain profiles with $\dot{a}$ =0 and n_2/n_1=1

It has been shown that wheel-ground contact angles can be estimated with common, low-cost sensors. As discussed below, this estimation is computationally simple, and thus suitable for on-board implementation.

3. Extended Kalman Filter Implementation

In the previous section the ground contact angles were expressed as functions of simple, measurable quantities. However, sensor noise will degrade these measurements, and wheel slip will further corrupt the estimate. In this section an Extended Kalman Filter (EKF) is developed to compensate for these effects.

3.1. EKF BACKGROUND

An Extended Kalman Filter is an effective framework for fusing data from multiple noisy sensor measurements to estimate the state of a nonlinear system (Brown, 1997). In the EKF framework the process and sensor signal noise are assumed to be unbiased Gaussian white-noise with known covariance. These are reasonable assumptions for the signals considered in this research.

Consider a given system with dynamic equations:

$$\dot{\mathbf{x}} = \mathbf{f}(\mathbf{x}, \mathbf{w}, \mathbf{v}, t) \tag{11}$$

where $\mathbf{w}$ and $\mathbf{v}$ represent measurement and process noise vectors. A linearized continuous-time state transition matrix can be defined as:

$$\mathbf{F} = \frac{\partial \mathbf{f}}{\partial \mathbf{x}}(\hat{\mathbf{x}}) \tag{12}$$

where $\hat{\mathbf{x}}$ is the current state estimate.
The system measurement vector $\mathbf{z}$ is defined as:

$$\mathbf{z} = \mathbf{h}(\mathbf{x}, \mathbf{v}) \tag{13}$$

with measurements are acquired at each time step *k*.

In general, computation of the EKF involves the following steps:

1. Initialization of the state estimate $\hat{\mathbf{x}}$ and a covariance matrix, $\mathbf{P}$.
2. Propagation of the current state estimate $\hat{\mathbf{x}}$ (from a discrete-time representation of Equation (12)) and covariance matrix $\mathbf{P}$ at every time step. The matrix $\mathbf{P}$ is computed as:

$$\mathbf{P}_k = \mathbf{F}_k \mathbf{P}_k \mathbf{F}_k^T + \mathbf{Q}_k \tag{14}$$

where $\mathbf{Q}$ is the system process noise matrix and is assigned based on the physical model of the system.

3. Updating the state estimate and covariance matrix as:

$$\hat{\mathbf{x}}_k = \hat{\mathbf{x}}_k + \mathbf{K}_k \left[\mathbf{z}_k - \mathbf{h}(\hat{\mathbf{x}}_k) \right] \tag{15}$$

and

$$\mathbf{P}_k = \left[\mathbf{I} - \mathbf{K}_k \mathbf{H}_k \right] \mathbf{P}_k \tag{16}$$

where the Kalman gain matrix **K** is given by:

$$\mathbf{K}_k = \mathbf{P}_k \mathbf{H}_k^T \left[\mathbf{H}_k \mathbf{P}_k \mathbf{H}_k^T + \mathbf{R}_k \right]^{-1} \tag{17}$$

where **R** is the measurement error covariance matrix and **H** is a matrix relating the state **x** to the measurement **z**.

3.2. EKF IMPLEMENTATION

For vehicle wheel-ground contact angle estimation, the EKF computes a minimum mean square estimate of the state vector $\mathbf{x} = \begin{bmatrix} a & \dot{a} & n_1 & n_2 & g_1 & g_2 \end{bmatrix}^T$. Since vehicle pitch can be measured and the wheel center speeds can be approximated from knowledge of the wheel angular velocities and radii, the EKF measurement vector is defined by $\mathbf{z} = \begin{bmatrix} a & n_1 & n_2 \end{bmatrix}^T$. Measurements are taken at every time step during vehicle motion.

The measurement error covariance matrix **R** is assumed to be diagonal. The elements of **R** corresponding to sensed quantities, such as the pitch and wheel center speeds, can be estimated by off-line measurement of the sensor noise. The elements of **R** corresponding to unmeasured quantities, such as the ground contact angles, can be computed by linearizing Equations (6) and (7) and summing the contributions of the measured noise terms.

Computation of the EKF (i.e. Equations (14) through (17)) involves several matrix inverse operations. However, it should be noted that the matrices involved are generally near-diagonal. Efficient inversion techniques can be used to reduce computational burden. Thus, EKF computation remains relatively efficient and suitable for on-board mobile robot implementation.

4. Simulation Results

A simulation was performed to observe the accuracy of ground contact angle estimation in the presence of noisy sensor signals. The EKF-

estimated ground contact angles were compared with the true ground contact angles.

The simulated system is a planar, two-wheeled vehicle traveling over undulating terrain (see Figure 4). The pitch a was corrupted with white noise of standard deviation 3°. This is approximately 10% of its range of values. It was assumed that the pitch rate $\dot{a}$ was computed from a. The rear and front wheel velocities, n_1 and n_2, were corrupted with white noise of standard deviation 0.02 cm/sec, which represents approximately 10% of its range of values. This simulates the error due to the combined effects of wheel slip and tachometer noise. In this simulation the wheel spacing distance l was 1 m.

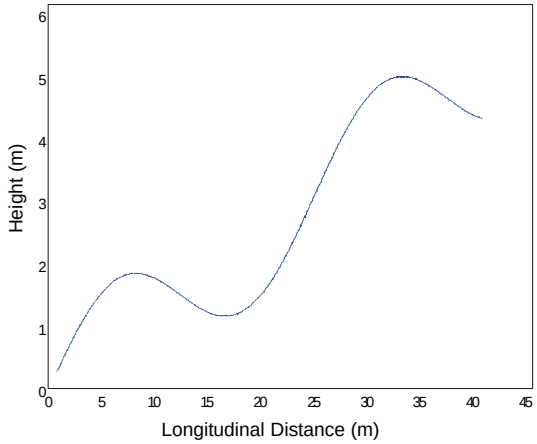

Figure 4. Simulated terrain profile

The EKF measurement covariance matrix was chosen based on the simulated sensor noise levels. The measurement covariances were chosen to be 150% of the simulated sensor noise levels in an attempt to emulate conservative human modeling of a physical rover system. The EKF should perform properly despite the imprecise covariance matrix. The EKF process noise matrix was chosen based on expected uncertainty sources such as wheel slip. Note that in practice, covariance estimates would be determined *a priori* from characterization of the physical sensors.

The results of the contact angle estimation simulation are shown in Figure 5. After an initial transient, the EKF estimate of the ground contact angle is quite accurate, with RMS errors of 1.60° and 1.65° for the front and rear contact angles, respectively. Error increases at flat terrain regions (i.e. where the slope of front and rear contact angles is identical) due to reasons discussed in Section 2. In general, the EKF does an excellent job of estimating wheel-ground contact angles in the presence of noise.

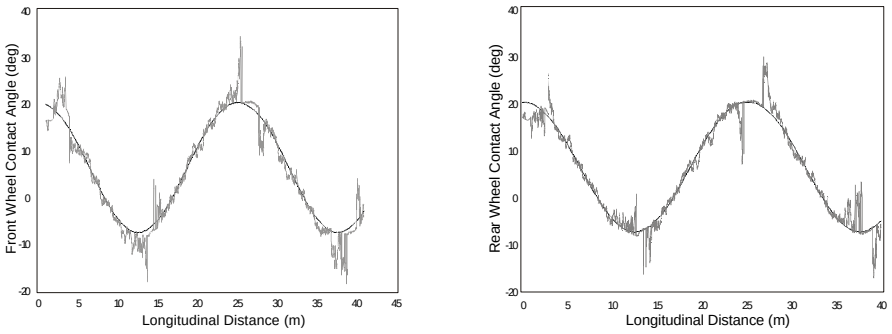

(a) Front Wheel *(b) Rear Wheel*

Figure 5. Actual (solid) and Kalman-filter estimated (gray) contact angles

5. Experimental Results

The EKF-based contact angle estimation algorithm has been implemented on the Field and Space Robotics laboratory six-wheeled microrover, shown in Figure 6 (Iagnemma *et al.*, 1999). The rover suspension is based on a six-wheeled rocker-bogey design, which has been used by NASA in such vehicles as Sojourner (Matijevic, 1997). Note that for this type of suspension, the contact angles for the front two wheels can be directly estimated with Equations (6) and (7). The rear wheel does not maintain a fixed distance from either the front or rear wheel, but does maintain a fixed distance to the bogey free-pivot joint and can thus be estimated. The rover features six independently powered wheels driven by geared DC motors. The resulting maximum velocity of the rover is approximately 8 cm/sec.

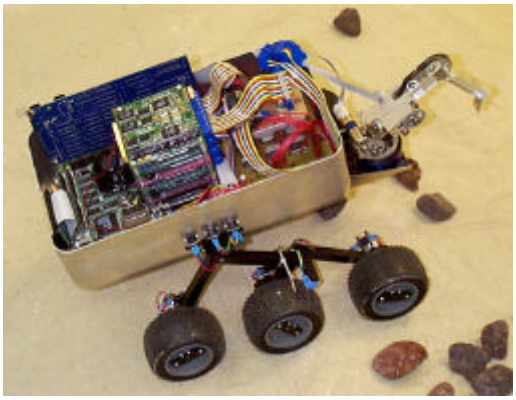

Figure 6. Field and Space Robotics Laboratory microrover

The measurement noise covariances for the EKF were estimated by analyzing sensor readings while the system was at rest. Process noise covariances were estimated based on results from the simulation.

The rover was driven from flat ground up a 20° incline, and the front and middle wheel-ground contact angles were estimated. The wheelbase length l of the front and middle wheels is 14 cm. Typical results of this experiment can be seen in Figure 7.

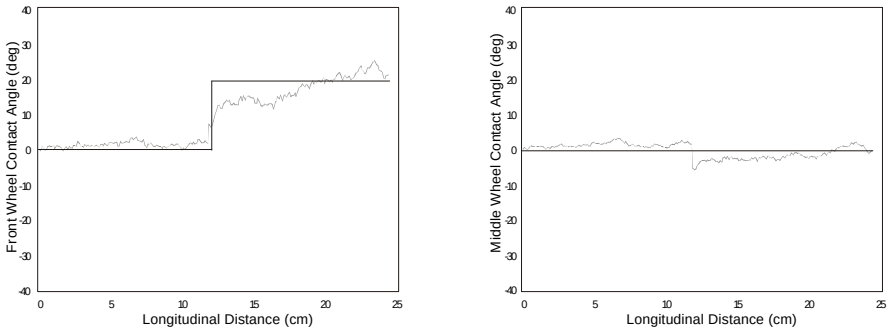

(a) Front Wheel *(b) Middle Wheel*

Figure 7. Actual (solid) and Kalman-filter estimated (gray) experimental results of FSRL rover traversing 20° incline

The estimate of the front wheel contact angle is approximately 20° while the middle wheel estimate remains at approximately 0°, since the middle wheel has not yet reached the incline. Thus we conclude that it is possible to accurately estimate the ground contact angles on a physical system with noisy sensors.

6. Conclusions and Future Work

This paper has presented a wheel-ground contact angle estimation algorithm based on rigid-body kinematic equations. The algorithm utilizes an extended Kalman filter to fuse on-board sensor signals. Simulation and experimental results on a six-wheeled rover have shown that the algorithm can accurately estimate wheel-ground contact angles in uneven terrain. The wheel-ground contact angle estimation algorithm is currently being integrated into a traction control system on a six-wheeled laboratory microrover.

Acknowledgements

The authors would like to thank Marco Meggiolaro of M.I.T. and Eric Baumgartner of the Jet Propulsion laboratory for their helpful contributions to this work.

References

Brown, R., and Hwang, P. (1997). *Introduction to Random Signals and Applied Kalman Filtering,* John Wiley and Sons.

Farritor, S., Hacot, H., and Dubowsky, S. (1998). "Physics-Based Planning for Planetary Exploration," *IEEE International Conference on Robotics and Automation*, pp. 278-83.

Hayati, S., Volpe, R., Backes, P., Balaram, J., and Welch, W. (1996). "Microrover Research for Exploration of Mars," *AIAA Forum on Advanced Developments in Space Robotics*.

Iagnemma, K., Burn, R., Wilhelm, E., and Dubowsky, S. (1999). "Experimental Validation of Physics-Based Planning and Control Algorithms for Planetary Robotic Rovers," *Proceedings of the Sixth International Symposium on Experimental Robotics, ISER '99.*

Matijevic, J., (1997). "Sojourner: The Mars Pathfinder Microrover Flight Experiment," *Space Technology,* Vol. 17, No. 3/4, pp. 143-149.

Mishkin, A., Morrison, J., Nguyen, T., Stone, H., Cooper, B., and Wilcox, B. (1998). "Experiences with operations and autonomy of the Mars Pathfinder Microrover," *Proceedings of the 1998 IEEE Aerospace Conference,* pp.337-51.

Sreenivasan, S., and Wilcox, B., (1994). "Stability and Traction Control of an Actively Actuated Micro-Rover," *Journal of Robotic Systems,* Vol. 11, no. 6, pp. 487-502.